Published: 21st November 2025

ANACHEM JOURNAL
ISSN: 2006-5221 (Online)

PERFORMANCE EVALUATION OF ACID-IMPREGNATED AND UNIMPREGNATED SOLID CATALYSTS IN THE PRODUCTION OF BIOFUEL FROM SELECTED LOCAL SEED OILS

[1*]Ndubuisi J.O., [2]Ekpunobi, U.E., [3]Umeokoli, B.O., [1]Ezeagwu, P.C., [2]Okonkwo, P.C., [2]Modozie, B.U., [2]Aghanwa, C.I. and [4]Princewill, O.A.

[1]Department of Biochemistry, Faculty of Basic Medical Sciences, Federal University of Allied Health Sciences Enugu State.

[2]Department of Pure and Industrial Chemistry, Faculty of Physical Sciences, Nnamdi Azikiwe University Awka.

[3]Department of pharmaceutical and Medicinal Chemistry, Nnamdi Azikiwe University Awka.

[4]Shanahan University Onitsha.

*Corresponding author's email: ndubuisijulie@gmail.com; abuchiokeke4@gmail.com

DOI:10.5281/zenodo.17625074

ABSTRACT

The desire for renewable and sustainable energy, coupled with the global demand for alternative energy sources that are not based on petroleum, has led to the increased popularity of biodiesel as an environmentally friendly substitute for petroleum diesel. To determine the efficiency of acid-impregnated and unimpregnated solid catalysts prepared using marine shells (*Pinctada margaritifera, Charonia tritonis,* and *Acanthocardia aculeata*) in the production of biodiesel using locally available seed oils of fluted pumpkin (*Telfairia occidentalis*), chia (*Salvia hispanica*), and pumpkin (*Cucurbita spp*.). This experiment compared the quality of the resulting biodiesel product with that of the biodiesel produced using the impregnated solid catalyst. Physicochemical characterization revealed that the oils differ in their acid value, viscosity, iodine value, and moisture content; hence, this influenced the suitability of these oils in direct transesterification. The fatty acid composition was determined using Gas Chromatography-Flame Ionization Detection (GC-FID). In contrast, the existence of ester carbonyls, aliphatic hydrocarbons, and unsaturated groups, which are characteristic of triglycerides, was confirmed using Fourier Transform Infrared Spectroscopy (FTIR). According to scanning electron microscopy (SEM), the porosity and surface roughness were enhanced by calcification. In contrast, the distribution of pores and crystallinity was improved by acid impregnation, which, in turn, enhanced the catalytic performance. Acid-impregnated catalysts outperformed unimpregnated catalysts in producing biodiesel with higher kinematic viscosity, flash point, and cloud point, which are physicochemical properties that better meet the ASTM D6751 standards. However, oxidative stability remained a weakness, and further refinement was necessary.

KEYWORDS: Biodiesel production, Heterogeneous catalysts, Acid impregnation, Local seed oils

1.0. INTRODUCTION

Global industrial growth, sustainable development, and improved quality of living are all driven by energy. Interest in renewable energy alternatives has increased due to rising global energy demand and concerns about environmental decline and the depletion of fossil fuel reserves. One of the most promising alternatives to traditional diesel is biodiesel, a sustainable fuel derived from biological sources. Its environmentally friendly qualities, biodegradability, and ability to be used in existing diesel engines without modification are drawing worldwide attention (Canaki and Sali, 2018). According to Ahmed *et al.,* (2021), biodiesel is the

mono-alkyl ester of long-chain fatty acids produced by trans-esterifying triglycerides with alcohols (typically ethanol or methanol). This process creates methyl or ethyl esters with properties similar to those of petroleum diesel, derived from vegetable or animal fats. Biodiesel is considered a viable fuel alternative for industrial and transportation applications due to its physicochemical properties, which include low sulfur content, a high octane number, and good lubricity (Chung *et al.,* 2019).

In contrast to fossil fuels, biodiesel contributes to environmental sustainability by reducing greenhouse gas emissions and other harmful pollutants. Based on the feedstock used, biodiesel manufacturing has evolved over the years and is divided into four generations. Edible vegetable oils such as corn, canola, sunflower, and soybean are used in the production of first-generation biodiesel; these oils often compete with food sources. By using inedible lignocellulosic biomass, such as husks, forest byproducts and agricultural leftovers, the second generation reduces the conflict between fuel and food (Elangara, 2015). While the fourth generation of biodiesel utilises genetically modified algae and cyanobacteria through synthetic biology techniques, the third generation is derived from algal biomass, which enables high lipid production (Khan, 2019).

Notwithstanding these developments, the cost and sustainability of feedstock remain a significant hurdle, and regional, inedible seed oils must be explored as an alternative source for biodiesel generation. Because they significantly improve the transesterification reaction by reducing activation energy and enhancing conversion efficiency, catalysts are key to the production of biodiesel. The three broad types of catalysts used in biodiesel production are homogeneous, heterogeneous, and biocatalysts. Although homogeneous catalysts are widely used in industries, they have significant disadvantages, including being non-reusable, requiring extensive purification, and generating waste (Sharma *et al.,* 2013). The benefits of heterogeneous catalysts are less environmental impact, ease of separation, and reusability. Due to their low cost and biodegradability, heterogeneous catalysts made from biomass are gaining increasing attention (Huang e*t al.,* 2012). Eggshells, bones, snail shells, and oyster shells are examples of locally produced materials that have shown promise as precursors for solid catalysts in the synthesis of biodiesel. Additionally, impregnating solid catalysts with acids makes them more porous, increases their surface area, and enhances their catalytic activity, which in turn increases the yield and quality of biodiesel (Pazouki *et al.,* 2010).

Compared to conventional fossil fuels, biodiesel has several advantages. It offers flexibility in fuel applications, as it can be used in any ratio with petroleum diesel (Bereczky and Torok, 2011). According to studies, biodiesel reduces air pollution and associated health hazards by reducing emissions of sulfur oxides, carbon monoxide, particulate matter, and unburned hydrocarbons (Marmesat *et al.,* 2017). Its renewable nature aligns it with the goals of the global energy transition, while its biodegradability ensures minimal environmental pollution in the event of spills.

Through transesterification using methanol in the presence of sodium hydroxide as a homogeneous catalyst, Ogbu and Ajiwe, (2016) demonstrated the potential of baobab seed oil as a renewable feedstock for biodiesel generation. Under optimal conditions of 60 ^{0}C, 30 W% methanol-to-oil ratio and 1.4 percent catalyst loading, the research yielded 96 W% biodiesel in less than an hour.

The limitations of homogeneous catalysts and the further improvement of biodiesel quality are demonstrated by the oxidative

stability, which fell below the ASTM D6751 regulations, despite the fuel's attributes being mainly in accordance with international norms. Heydarzadeh *et al.,* (2010) examined the range of plant and animal-based feedstock that can be utilized to produce biodiesel and observed that the industry has overcome some obstacles to meet the growing demand for biodiesel, thanks to advancements in processing technologies.

The study highlighted the need for alternative, non-edible feedstock by emphasizing the reliance on edible oils and the persistent issue of high production costs. Fatty acid methyl esters (FAME) and glycerin are byproducts of the transesterification of oils with alcohol in the presence of a basic catalyst, according to Ogbu and Ajiwe, (2013). However, they also noted that purification is necessary to meet international standards for biodiesel quality. These studies demonstrate both the progress and limitations of homogeneous catalyst-based biodiesel production. They support the analysis of heterogeneous solid catalysts, especially acid-impregnated and unimpregnated types, using local resources as sustainable alternatives that have the potential to improve the qualities of biodiesel from native seed oils, thereby reducing costs and enhancing catalytic performance.

The effectiveness in the synthesis of biodiesel from certain local seed oils, fluted pumpkin (*Telfairia occidentalis*), chia seed (*Salvia hispanica L*.) and pumpkin (*Cucurbita spp*.) of acid-impregnated and unimpregnated solid catalysts is investigated in this study. To prepare solid catalysts, marine shell wastes such as *Pinctada margaritifera, Charonia tritonis,* and *Acanthocardia aculeata* are used as precursors. The process includes the characterization of the synthesized biodiesel and catalysts and the optimization of reaction parameters such as catalyst concentration, temperature, time, alcohol/oil molar ratio and agitation speed.

2.0. MATERIALS AND METHODS

2.1 Materials and chemicals

Feedstocks included local pumpkin seed oils, chia seed oils, and fluted pumpkin. Catalysts were made using marine shells (*Pinctada margaritifera, Charonia tritonis and Acanthocardia aculeate*). Sodium hydroxide, methanol and n-hexane were taken as analytical-grade chemicals. Glassware and equipment included beakers, separating funnels, Soxhlet extractors, rotary evaporators, muffle furnaces, ovens, hotplates with magnetic stirrers, viscometers and spectroscopic analysis instruments used to characterize them.

2.2. Oil Extraction

The seeds were dried, cleaned, and crushed. Each seed sample underwent Soxhlet extraction with 1200 mL of n-hexane as the solvent. A rotary evaporator was used to remove the solvent under reduced pressure to obtain the crude oil. The oil yield was calculated as:

$$\%\ \text{Oil extracted}ti = \frac{\text{weight of oil extracted} \times 100}{Weight\ of\ sample\ used}.$$

2.3. Catalyst Preparation

The shells, having been collected, were cleaned, dried, and pounded into a fine powder. The next step involved the calcination of the powder (two hours at 900 ^{0}C in a muffle furnace). An adequate powdered catalyst, suitable for biodiesel production, was obtained through the cooling process, followed by further crushing and sieving of the resultant ash. To enhance the surface acidity and catalytic activity of the acid-impregnated catalysts, the calcined ash was treated with the appropriate acid solution, dried, and then re-calcined.

2.4. Biodiesel Synthesis via Transesterification

The transesterification process was performed in a 500 mL batch reactor equipped with a magnetic stirrer and a reflux condenser. Fifty millilitres of preheated (65 °C) seed oil were added to a pre-mixed solution of 65 °C methanol and solid catalyst (calcium methoxide). The molar ratios of methanol to oil ranged from 2:1 to 6:1, the catalyst loading was between 0.5% and 1.5%

(w/w), and the reaction was conducted at 250 rpm for 45 to 75 minutes. Afterwards, the mixture was transferred to a separating funnel and left to settle for one hour, allowing the glycerol (bottom layer) to separate from the biodiesel (top layer). The recovered biodiesel was dried to remove all remaining water and methanol. The calculation of the biodiesel yield was as follows:

$$\%Yield = \frac{\text{Weight of Fatty Acid Methyl Ester} \times 100}{\text{Weight of Oil Used}}$$

2.5 Characterization of Oils and Biodiesel

2.5.1 Physicochemical Characteristics

According to the standards of the American Society for Testing and Materials (ASTM) guidelines, the density, specific gravity, kinematic viscosity, acid value, free fatty acid content, saponification value, iodine value, moisture content, flash point, cloud point, and pour point of extracted oils and obtained biodiesel were studied.

2.5.2 Spectroscopic and Chromatographic Analysis

Fourier Transform Infrared Spectroscopy (FTIR) was utilized to identify the functional groups in the oils and biodiesel. Gas Chromatography with flame ionization detection (GC-FID) was employed to analyse the composition of fatty acids.

2.5.3 Catalyst Characterization

The shape and surface structure of the solid catalysts were analyzed by Scanning Electron Microscopy (SEM). The elemental composition was studied using X-ray Fluorescence (XRF).

2.6 Experimental Design and Optimization

A Central Composite Design (CCD) was used to examine the effects of temperature, reaction time, catalyst concentration, and methanol-to-oil ratio on biodiesel yield. Thirty experimental runs were carried out, and the results were analyzed using Design of Experiments software. The response variable (FAME content) was related to the independent variables by a second-order polynomial model.

$$Y = b0 + \Sigma ki = 1bixi + \Sigma ki = 1bi\, xi2 + \Sigma ki = 1 + \Sigma ki = jbij\, xi\, xj + e$$

Where Y is the biodiesel yield, b_0 is the intercept, b_i, b_{ii}, and b_{ij} are regression coefficients, X_i and Xj are independent variables, and e is random error. Analysis of variance (ANOVA) was used to assess the significance of model terms.

3.0 Results and Discussion

3.1 Characterization of the oil samples

The three oil types in Table 1, which were studied for their physicochemical properties, were compared to the ASTM standard requirements for biodiesel feedstock (DFS), and significant differences were observed. The moisture content of oil C was 1.92, of oil A, 7.84 and of oil B, 7.84. These figures were significantly lower than the ASTM D6751 maximum requirement of 0.05%. Since they promote hydrolysis and microbial degradation, which can increase the acid value of the oil and lead to poor performance in the transesterification process, a high moisture content is undesirable.

The specific gravities of the oils ranged between 0.831 and 1.040, which is slightly higher than the 0.86-0.90 range recommended by ASTM D6751. Although the value of Oil A (1.040) was above the expectations, Oil B (0.831) was under the limit, which could indicate impurities or variation in the level of unsaturation. The saponification values of the samples differed significantly. The values of Oil B and Oil C were 129.03 and 162.69 mEq/KOH, respectively, and the value of Oil A was extremely high, i.e. 8964.78 mEq/KOH. These results differ significantly from traditional expectations, as ASTM D6751 does not specify a fixed saponification value. However, when a steady production of biodiesel is required, moderate values are often recommended. The existence of shorter-chain fatty acids, which can influence fuel stability, is indicated by the extremely high value of Oil A.

The peroxide value of the oil was the highest (48 mEq/g) in Oil A, the middle peroxide value was 36 mEq/g, and the lowest peroxide value was 12 mEq/g in Oil A and B, respectively. All the oils were within acceptable limits, according to ASTM D6751, which stipulates that the peroxide values must be less than 125 mEq/g. Nevertheless, the higher peroxide value of Oil A suggests that it is more susceptible to oxidative deterioration and rancidity. Oil A contained a much higher iodine value (296.18 mEq/g) than the iodine value in Oil B (22.59 mEq/g) and Oil C (16.37 mEq/g). ASTM D6751 has a limit of 125 mEq/g. This implies that the compliance of Oils B and C was better. In contrast, Oil A contains a high proportion of unsaturated fatty acids, making it susceptible to oxidation and polymerisation during storage.

The acid value had a significant difference. Oil B showed 0.168 mEq/KOH, Oil C 20.196 mEq/KOH, and Oil A 3.927 mEq/KOH. ASTM recommends a limit of 0.05 mEq/KOH. This means that Oils A and C should undergo pretreatment (esterification) to reduce the concentration of free fatty acids and facilitate biodiesel production, while Oil B should be used in direct transesterification. Kinetic viscosity at 40 degC was very high in Oil A (10 802 mPa s) than in Oil B (95.86 mPa s) and Oil C (180.97 mPa s). The ASTM standard specifies a viscosity range of 1.9-6.0 mPa·s, indicating that none of the oils met the requirements. The high viscosity may interfere with the ability to atomize fuel and the combustion efficiency of the engines; therefore, viscosity reduction should be practiced in handling biodiesel. The value of refractive index was between 1.445 and 1.452 within the acceptable range of reported values of vegetable oils with the presence of conjugated double bonds and saturation levels.

The flash points of the oils exceeded the ASTM minimum of 130 °C, ranging from 230 °C to 250 °C. This helps to achieve excellent safety traits during handling and storage since the flash points are reduced, and thus fire threats are reduced. The cloud point of oil A (1 °C), B (5 °C) and C (8 °C) have varied values. Similarly, the pour point of Oil A was 7 °C, Oil B was 10 °C, and the pour point of Oil C was 8 °C. In colder climates, Oils B and C may be problematic; however, these values tend to fall within the range of -3 to 12 °C cloud point and -15 to 10 °C pour point, as specified by ASTM, indicating sufficient cold flow quality in these oils.

Table 1.0: Physicochemical Properties of the Raw Oils Compared with ASTM D6751 Standard

Parameter	Oil A	Oil B	Oil C	ASTM D6751 Standard
Moisture Content (%)	7.84	7.84	1.92	0.05 (Max)
Specific Gravity	1.040	0.831	0.875	0.86 – 0.90
Saponification Value (mg KOH/g)	8964.78	129.03	162.69	-
Peroxide Value (mEq/g)	48	12	36	< 125
Iodine Value (mEq/g)	296.18	22.59	16.37	0 – 120
Acid Value (mg KOH/g)	3.927	0.168	20.196	0.05 Max
Kinematic Viscosity @ 40°C (mm^2/s)	10802	95.86	180.97	1.9 – 6.0
Refractive Index	1.445	1.452	1.448	-
Flash Point (°C)	230	240	250	130 (Min)
Cloud Point (°C)	1.2	5.0	8.0	-3 to 12
Pour Point (°C)	7.0	10.0	8.0	-15 to 10

3.2 Fatty acid composition of the three oil samples

Lauric acid (12:0, 12.62%), Myristic acid (14:0, 10.24%), Palmitic acid (16:0, 10.36%), Stearic acid (18:0, 10.28%), Arachidic acid (20:0, 10.90%), Docosadienoic acid (22:2, 10.74%) are the main fatty acids in Raw Sample A. Also, unsaturated fatty acids were identified, including oleic acid (18:1, 9.93%), linoleic acid (18:2, 8.53%), and docosahexaenoic acid (22:6, 9.11%). Sample A was the only one that contained capric acid (10:0, 7.29%). A greater percentage of the composition of Raw Sample B is unsaturated fatty acids. The central portions are myristoleic acid (14:1, 13.89%), palmitoleic acid (16:1, 11.27%), margaric acid (17:0, 11.39%), eicosatetraenoic acid (20:4, 11.99%), as well as docosahexaenoic acid (22:6, 11.82%). Saturated fatty acids described as myristic acid (14:0, 8:02, not present in this sample), stearic acid (18:0, 10.38%) and lauric acid were also identified, but in lower amounts as compared to the unsaturated ones. The profiles of the Raw Samples C and B were quite close in terms of the fact that the quantities of the major fatty acids were practically identical. Myristoleic acid (14:1, 13.89%), Palmitoleic acid (16:1, 11.27%), Margaric acid (17:0, 11.39%), Oleic acid (18:1, 11.32%), Linoleic acid (18:2, 10.93%), Eicosatetraenoic acid (20:4, 11.99%), and Docosahexaenoic acid (22:6, 9.10%). The fact that Samples B and C were more similar than Sample A indicates there is a possibility that they might have been produced by the same or a more similar source, as opposed to Sample A which showed a more diversified diversity of fatty acids, in particular, the medium and long-chain fatty acids which were not detected in Sample B and C: Capric acid (10:0) and Lauric acid (12:0). This means that Samples B and C may contain more essential fatty acids that may have potential health benefits. Still, Sample A may be more stable and rich in energy-dense properties.

Table 2.0: Result of fatty acid composition

S/N	Fatty Acid	Carbon Number	% Weight (A)	Carbon Number	% Weight (B)	Carbon Number	% Weight (C)
1	Capric acid	10:0	7.2875	-	-	-	-
2	Lauric acid	12:0	12.6218	-	-	-	-
3	Myristic acid	14:0	10.2405	14:0	8.0171	14:0	8.0171
	Myristoleic acid	14:1	-	14:1	13.8856	14:1	13.8856
4	Palmitic acid	16:0	10.3577	-	-	-	-
	Palmitoleic acid	16:1	-	16:1	11.2667	16:1	11.2667
	Margaric acid	17:0	-	17:0	11.3947	17:0	11.3947
5	Stearic acid	18:0	10.2839	18:0	10.3788	18:0	10.3788
6	Oleic acid	18:1	9.9302	18:1	11.3190	18:1	11.3190
7	Linoleic acid	18:2	8.5251	18:2	10.9271	18:2	10.9271
8	Arachidic acid	20:0	10.8991	-	-	-	-
	Eicosatetraenoic acid	20:4	-	20:4	11.9904	20:4	11.9904
9	Docosadienoic acid	22:2	10.7448	-	-	-	-
10	Docosahexaenoic acid (DHA)	22:6	9.1094	22:6	11.8206	22:6	11.8206

3.3 FTIR characterization of oil

The Fourier Transform Infrared (FTIR) spectra of Tables 3, 4 and 5 indicate the different distributions of functional groups in the three raw oils (A, B and C). The characteristic absorption bands at around 1743 cm^{-1} of Table 3 (Oil A) are the stretching vibrations of the ester carbonyl group (C=O). The potential of the oil as a feedstock for the production of biodiesel is confirmed with this feature of triglycerides. The broad band at 3450 cm^{-1} is attributed to the stretching of hydroxyl (O-H) groups, which could be induced by residual moisture or free fatty acids in the oil. Detection of long hydrocarbon chains typical for fatty acids is confirmed by the bands in the range of 2850 to 2922 cm^{-1} corresponding to the C-H stretching vibrations of aliphatic $-CH_2$ and $-CH_3$ groups. The ester composition of the oil is indicated by peaks at 1160-1240 $cm^{-1,}$ which correspond to C-O stretching vibrations. Similar functional groups were observed in the FTIR spectrum of Table 4 (Oil B); however, minor variations in peak intensity and location indicated variations in the fatty acid composition. The ester carbonyl group is again indicated by a strong absorption at 1741 cm^{-1}, while aliphatic C-H stretching vibrations are indicated by absorption peaks at 2852-2925 cm^{-1}. The presence of cis-olefinic =C-H stretching, which implies unsaturated fatty acids, is indicated by the absorption at about 3005 cm^{-1}.

In comparison to Oil A, the broad O-H stretching band at 3460 cm^{-1} was weak, which was indicative of reduced moisture or free fatty acid concentration. The triglyceride backbone was further confirmed by the presence of peaks at 720 cm^{-1}, which were attributed to the rocking vibration of the long-chained methylene groups. The FTIR spectrum in Table 5 (Oil C) also revealed the bands at 2850-2921 cm^{-1} of C-H stretching vibrations, and high absorption of 1744 cm^{-1} of ester carbonyl stretching. In comparison to Oils A and B, a distinct absorption at 3010 cm^{-1} indicated a higher degree of unsaturation, which would indicate a higher percentage of double bonds in its fatty acid chains.

The comparably low acid value determined in the physicochemical examination is consistent with the weak O-H stretching absorption, which is a suggestion of few free fatty acids. The predominance of triglycerides was verified by the absorptions in the region 1165-1245 cm^{-1}, which corresponded to the stretching vibrations of C-O-C double bonds. The necessary functional groups present in vegetable oils, i.e. ester carbonyl, aliphatic hydrocarbons and unsaturated double bonds, were all observed in the spectra of Oils A, B and C. However, compositional changes in fatty acid profiles are reflected in changes in intensities and locations of absorption. In accordance with its higher acid and peroxide values, oil A exhibited a higher O-H stretching frequency, indicating a higher free fatty acid and moisture content. Oil B showed moderate unsaturation, and Oil C had the highest degree of unsaturation as demonstrated by the large olefinic C-H stretching.

Table 3.0: FTIR Interpretation of Raw Oil Sample A

Wavenumber (cm^{-1})	Intensity	Functional Group / Compound	Vibration Mode
3690.44	Strong	OH in alcohols and phenols	OH stretch
3497.37	Medium-Strong	NH in aromatic amines, primary amines & amides	NH stretch

Wavenumber (cm^{-1})	Intensity	Functional Group / Compound	Vibration Mode
3296.73	Strong	NH in secondary amides, polypeptides & proteins	NH stretch
3178.89	Very broad	NH_3^+ in amino acids	NH_3^+ antisymmetric stretch
3078.03	Medium	=CH–H in aromatic acids, unsaturated hydrocarbons	=CH–H stretch
1830.98	Strong	C=O in β-lactones	C=O stretch
1704.98	Strong	C=O in ketones	C=O stretch
1621.67	Strong	C=O and NH_2 (primary amides)	C=O stretch, NH_2 deformation
1467.79	Very strong	CH_2 in aliphatic compounds	CH_2 scissoring vibration
1297.55	Very strong	N–O of pyridine N-oxide	N–O stretch
1145.01	Strong	SO_2NH_2 in sulfonamides	SO_2 symmetric stretch
1018.09	Strong	C–O–H in cyclic alcohols	C–O stretch
842.93	Medium	C–Cl in chloro compounds	C–Cl stretch

Table 4.0: FTIR Interpretation of Raw Oil Sample B

Wavenumber (cm^{-1})	Intensity	Functional Group / Compound	Vibration Mode
3695.99	Strong	OH in alcohols and phenols	OH stretch
3385.06	Medium-Strong	NH in aromatic amines, primary amines & amides	NH stretch
3178.89	Very broad	NH_3^+ in amino acids	NH_3^+ antisymmetric stretch
2901.91	Medium-Strong	$–CH_3$ and $–CH_2$ in aliphatic compounds	CH antisymmetric & symmetric stretch
2593.19	Weak	–SH in alkyl mercaptans	S–H stretch
2099.48	Medium	N=N=N in azides	N=N=N stretch
1830.76	Strong	C=O in β-lactones	C=O stretch
1623.61	Weak-Medium	NH in primary amides	NH deformation
1455.04	Very strong	CH_2 in aliphatic compounds	CH_2 scissoring vibration
1365.01	Strong	NO_2 in aliphatic nitro compounds	NO_2 stretch

Table 5.0: FTIR Interpretation of Raw Oil Sample C

Wavenumber (cm^{-1})	Intensity	Functional Group / Compound	Vibration Mode
3497.37	Medium-Strong	NH in aromatic amines, primary amines & amides	NH stretch
3347.47	Medium	NH_2 in primary amides	NH_2 antisymmetric stretch
3253.88	Medium-Strong	≡CH in acetylenes	≡CH stretch

Wavenumber (cm^{-1})	Intensity	Functional Group / Compound	Vibration Mode
2976.12	Medium-Strong	$–CH_3$ and $–CH_2$ in aliphatic compounds	CH antisymmetric & symmetric stretch
2867.66	Medium	$–CH_2$ in aliphatic compounds	CH stretching
2730.66	Weak-Medium	CHO in aldehydes	Overtone of CH bending
2230.86	Medium	N≡N in diazonium salts	N≡N stretch
1986.08	Strong	C=C=C in allenes	C=C=C stretch
1854.94	Strong	C=O in β-lactones	C=O stretch
1730.03	Strong	C=O in δ-lactones	C=O stretch
1608.97	Strong	NH_2 in amino acids	NH_2 deformation (broad)
1409.33	Medium	C–N in primary amides	C–N stretch
1142.19	Strong	SO_2 in sulfones	SO_2 symmetric stretch
1019.75	Weak	Carbon ring in cyclic compounds	Ring vibration
766.03	Medium	C–S in sulfonyl chloride	C–S stretch

3.4 Catalyst Characterization

Using Scanning Electron Microscopy (SEM) examination, the structural and morphological properties of the raw, calcined and acid-activated catalysts were studied. The raw, calcined and acid-activated catalysts are represented in the form of SEM micrographs in Figures 1a-c, 2a-c and 3a-c, respectively. The micrographs of the raw catalysts revealed comparatively dense surfaces with few pores, indicating a compact arrangement of the particles. The morphology changed dramatically during calcination at 900°C, with a higher granularity and interconnected micropores. The breakdown of organic materials and the loss of volatile components during heating, which increases the accessible surface area, are responsible for this transition. Compared to the calcined samples, the acid-activated catalysts exhibited a much more defined pore network and roughened surface, indicating that the acid treatment further improved the porosity and surface texture. During transesterification, these textural enhancements increase the adsorption of reactant molecules and catalytic activity.

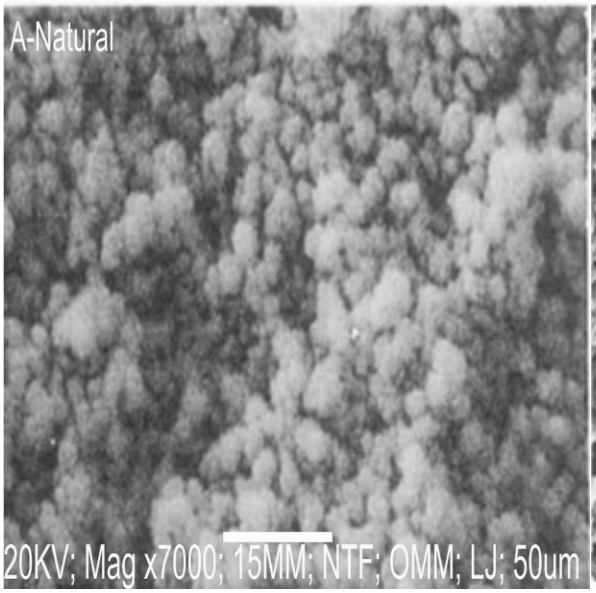

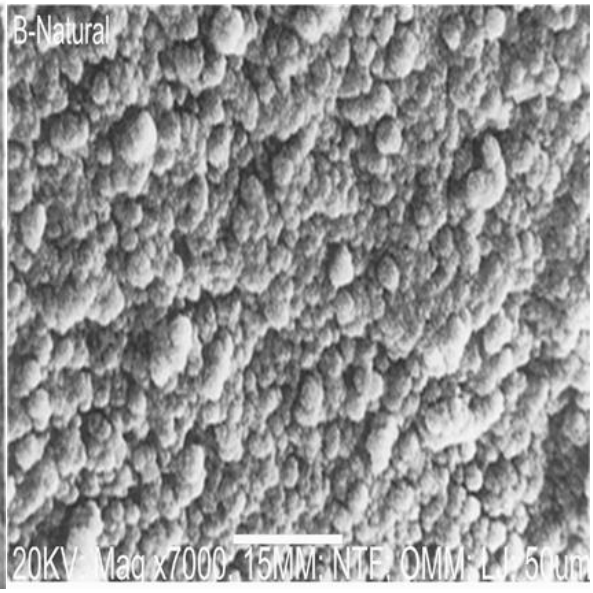

Figure 1a: **The result for Scanning Electron Microscope (SEM) of raw catalyst A.**
Figure 1b: **The result for Scanning Electron Microscope (SEM) of raw catalyst B.**

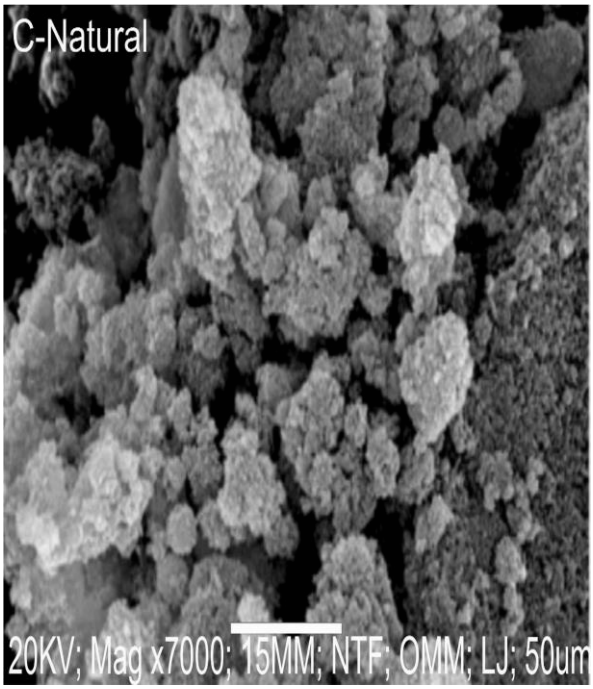

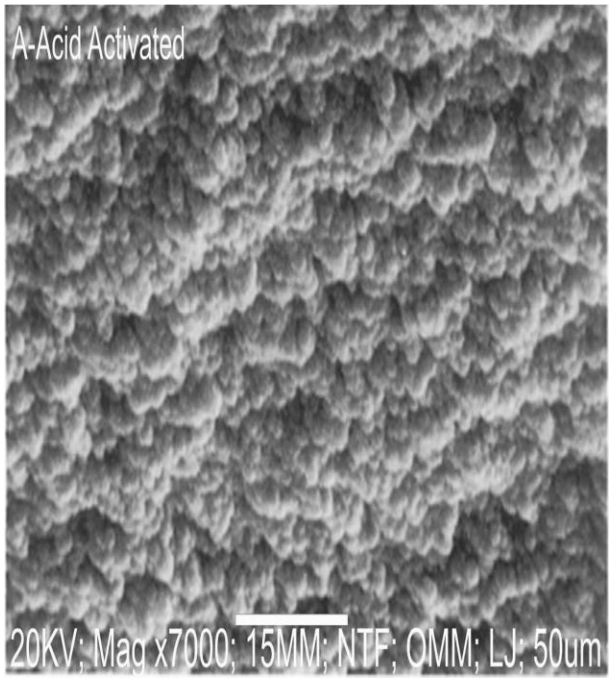

Figure 1c: the result for Scanning Electron Microscope (SEM) of raw catalyst C.
Figure 2a: the result for Scanning Electron Microscope (SEM) of acid activated catalyst A.

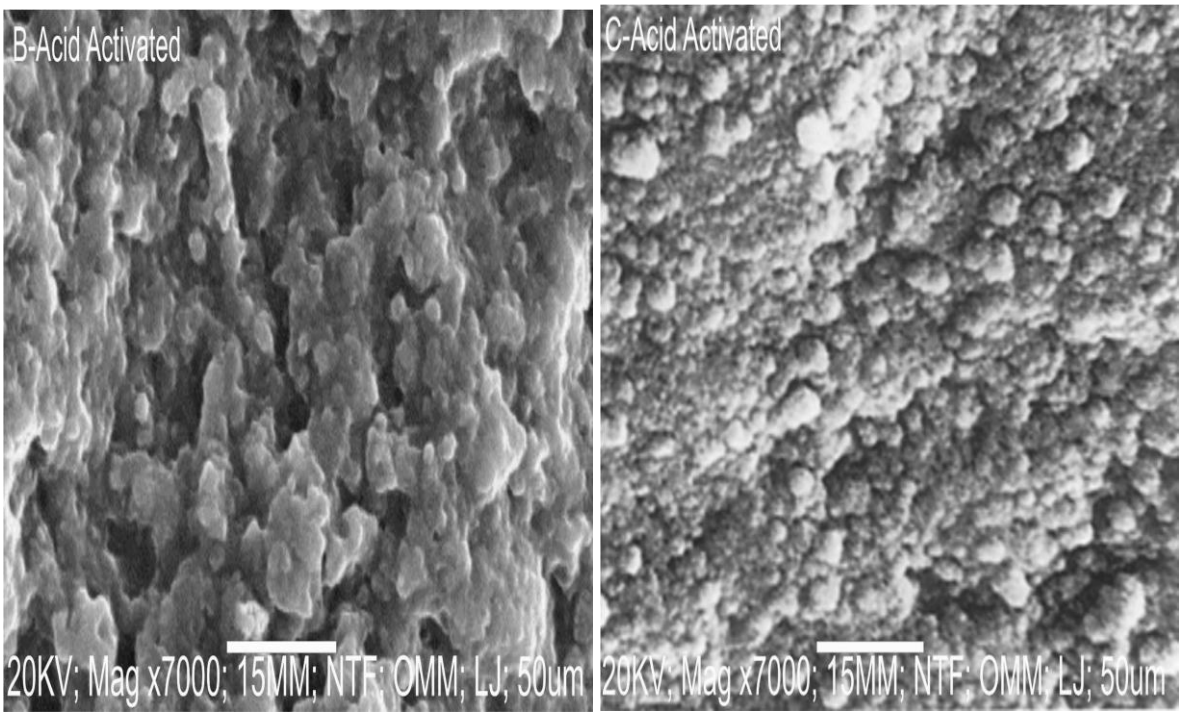

Figure 2b: **the result for Scanning Electron Microscope (SEM) of acid activated catalyst B.**
Figure 2c: **the result for Scanning Electron Microscope (SEM) of acid activated catalyst C.**

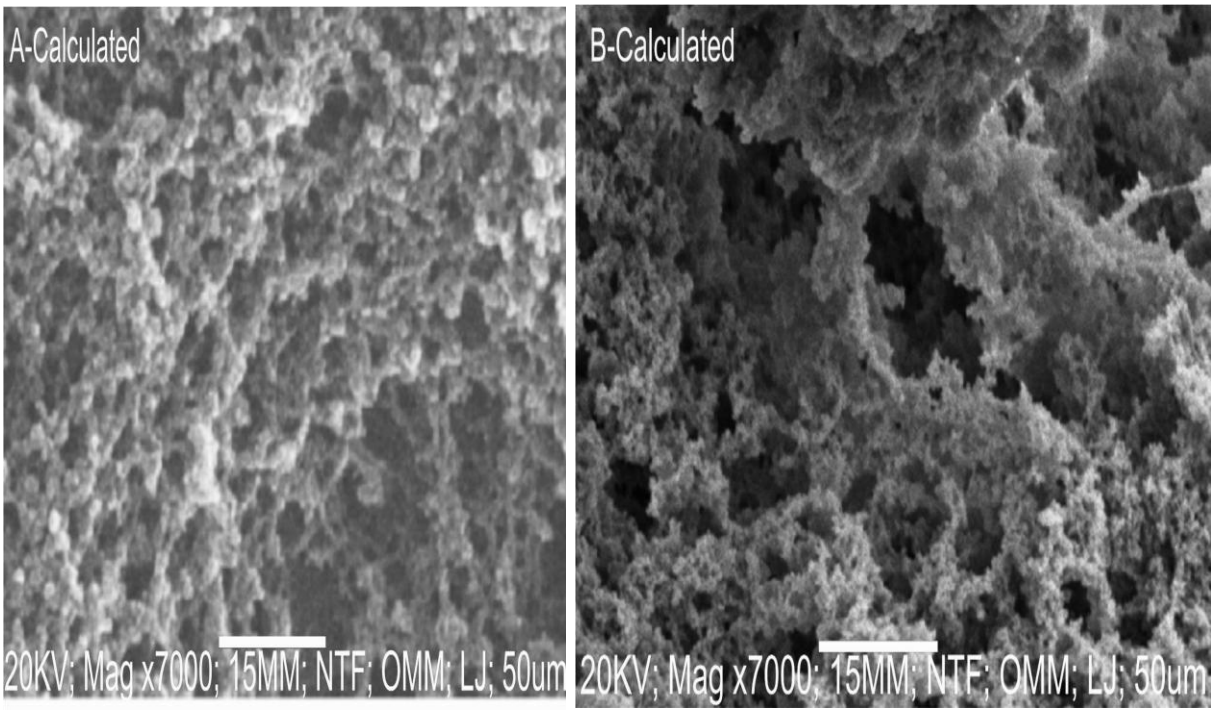

Figure 4.3a: **the result for Scanning Electron Microscope (SEM) of Calcinated catalyst A.**
Figure 4.3b**:** the result for Scanning Electron Microscope (SEM) of Calcinated catalyst B

.

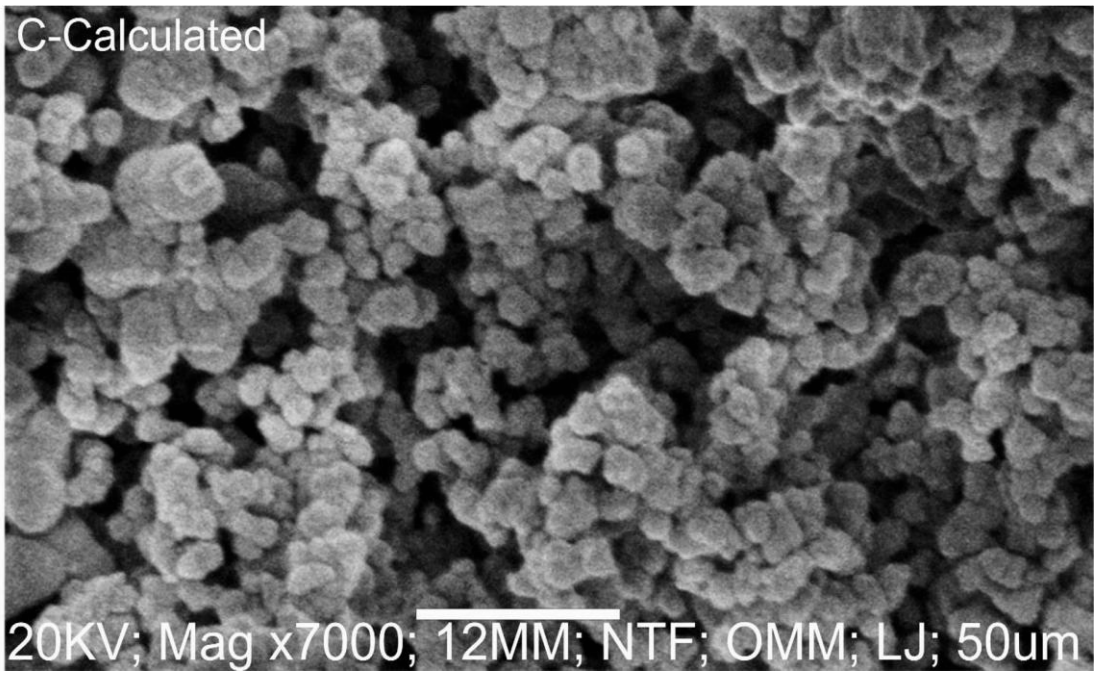

Figure 4.3c: **the result for Scanning Electron Microscope (SEM) of Calcinated catalyst C.**

4.0. CONCLUSION

Using heterogeneous catalysts, this paper demonstrated the potential of locally available seed oils (A, B, and C) as suitable feedstocks for biodiesel production. The Soxhlet process was employed to extract the oils, which had physicochemical properties indicative of triglyceride-rich structures. Changes in essential parameters such as acid value, iodine value, and kinematic viscosity indicated that pretreatment was necessary to optimize their suitability for transesterification. Molecular characterisation, confirmed by FTIR spectral analysis, revealed the presence of unsaturated bonds, aliphatic hydrocarbons, and ester carbonyl groups—key indicators of oils suitable for blending with biodiesel. SEM analysis of the catalysts showed that they were produced using natural precursors, which were calcined and acid-impregnated to enhance their porosity, crystallinity, and CaO content upon activation. These improvements increased catalytic efficiency, resulting in better conversion of oil to fatty acid methyl esters (FAME). Although oxidative stability needs to be improved, the produced biodiesel's performance largely aligns with the acceptable ranges of ASTM D6751 standards.

REFERENCES

Ahmed, A., Elkatatry, S. and Al-Afran, S. (2021). Application of biodiesel indrilling fluids. *Geo Fluids,* 37(16): 1011-1023.

Bereczky, A. and Torok, A. (2011). International literature review on the production. Possibilities of Biodiesel Transportation Engineering, 39(1): 31-37.

Canakci, M. and Sali, H. (2018). Biodiesel production for various feedstocks and their effects of the fuel properties. Journal of Indian Microbiohol, Biotechnoloty, 33: 1431-1441.

Chung, Z.I., Tan, Y.H., Chan, Y.S., Kansedo, J., Mukarak, N.M., Ghasemi, M., and Abdullah, M.O. (2019). Life cycle assessment of waste cooking oil for biodiesel producing using waste chicken egg shell derived cao as a catalyst via

transesterification. *Biocatalysts and Agricultural Biotechnology*, 21, 101317.

Elangaran, T. (2015). Biodiesel and its properties from using feed stocks restaurant. *Journal for Trends in Engineering and Technology,* 1(2): 15-21.

Heydarzadeh, J.K. Amini, G. Khalizadeh, M.A. Pazouki, M. Ghoreyshi, A.A. Rabeai M. and Najafpour, G.D. (2010).Esterification of Free Fatty Acids by Heterogeneous - Alumina-Zirconia Catalysts for Biodiesel Synthesis.*World Applied Sciences Journal*, 9(11), 1306-1312.

Huang, D., Zhao, H. and Lin, L. (2012). Biodiesel: an alternative to conventional fuel energy procedia, 16: 1874-1885.

Khan, S. (2019). Prospects of biodiesel production from microalgae in India. *Renewable and Sustainable Energy Reviews,* 13: 2361-2372.

Marmesat, S., Rodnqvez, E., Velasco, J., and Dorbangarnes, M.C. (2017). Used frying fats and oils: comparison of rapid tests based on chemical and physical properties biodiesel production. *International Journal of Food Science and Technology,* 42: 601-608.

Ogbu, I.M. and Ajiwe, V.I.E. (2013). Biodiesel production via esterification of free fatty acids from cucurbita peppo L. seed oil: kinetic studies. *International Journal of Science and Technology,* 2(8), 616-621.

Ogbu, I.M. and Ajiwe, V.I.E. (2016). Fuel properties and their correlations with fatty acids structures of methyl-and butyl-esters of Afzelia Africana, cucurbita peppo and Hura crepitans seed oils. *Waste and Biomass Volorization,* 7, 373-381.

Pazouki, M. Zamani, F. Zamzamcan, A.H. Fahar, M. and Najafpour, G. (2010). Esterification of Free Fatty Acids by Rhizopus Oryzae as Cell-Catalyzed from Used Cooking Oil for Biodiesel Production.*World Applied Sciences Journal,* 8(6), 719-724.

Sharma, V. and Sumbali, G. (2013).An Overview of the Symbiotic Interaction between Ants, Fungis and Other Living Organisms in Ant-Hill Soil. *International Journal of Environmental Science,* 4(3), 432-443.